Pergamon

International Journal of Machine Tools & Manufacture 38 (1998) 827–842

INTERNATIONAL JOURNAL OF
MACHINE TOOLS
& MANUFACTURE
DESIGN, RESEARCH AND APPLICATION

An analysis of drawbead restraining force in the stamping process

Fuh-Kuo Chen*, Pao-Ching Tszeng

Department of Mechanical Engineering, National Taiwan University, Taipei, Taiwan, R.O.C.

Received 1 October 1996; in final form 7 July 1997

Abstract

A theoretical model based on the virtual work principle was proposed to calculate the restraining force produced by the drawbead located on a stamping die surface. In the theoretical model the deformation of the sheet metal drawn over the groove shoulder or bead is assumed to be subjected to bending, sliding and unbending processes, and only the sliding process is responsible for the frictional force. The governing equations derived from the theoretical model were solved by a numerical procedure. In order to validate the proposed model, the finite element simulations were also performed to calculate the drawbead restraining forces for various steels. The simulated results together with the experimental data obtained from the published literature were compared with the predicted values calculated by using the numerical procedure. The good agreement between the simulated results, experimental data and the calculated values justifies the proposed theoretical model.

Keywords: Drawbead; Restraining force; Stamping; Energy method

1. Introduction

In a stamping process, a sheet metal is first clamped by the binders around the periphery of the die cavity and is subsequently drawn into the die cavity by a moving punch to form the

* Corresponding author.

0890-6955/98/$19.00
PII: S0890-6955(97)00048-5

desired shape, as shown in Fig. 1 [1]. The amount of the sheet metal moving into the die cavity is usually controlled by the frictional force generated between the binders and the sheet metal. For some stamping operations, the restraining force provided by the friction alone is not enough to control the metal-flow, and drawbeads are therefore added to the binders for reinforcement. The drawbead consists of a small groove on the die surface matched by a bead on the binder surface, as shown in Fig. 1. When it is drawn over the drawbead after the binder closure, the sheet metal is subjected to a bending and a subsequent unbending around the entry groove shoulder, and a repeated sequence at the bead and at the exit groove shoulder, as shown in Fig. 2. These bending and unbending deformations together with the frictional force account for the drawbead restraining force.

The magnitude of the restraining force is very important to the part formability in a stamping practice. For a shallow stamped part, such as a car roof, a large restraining force is required to deform the central area of the part, while a large restraining force will lead to fracture in a deep drawn part. Therefore, quite a few efforts have been focused on the study of the drawbead restraining force. In order to measure the drawbead force, Nine [2] designed a drawbead simulator and conducted a series of experiments on various steels and aluminum alloys. He also replaced

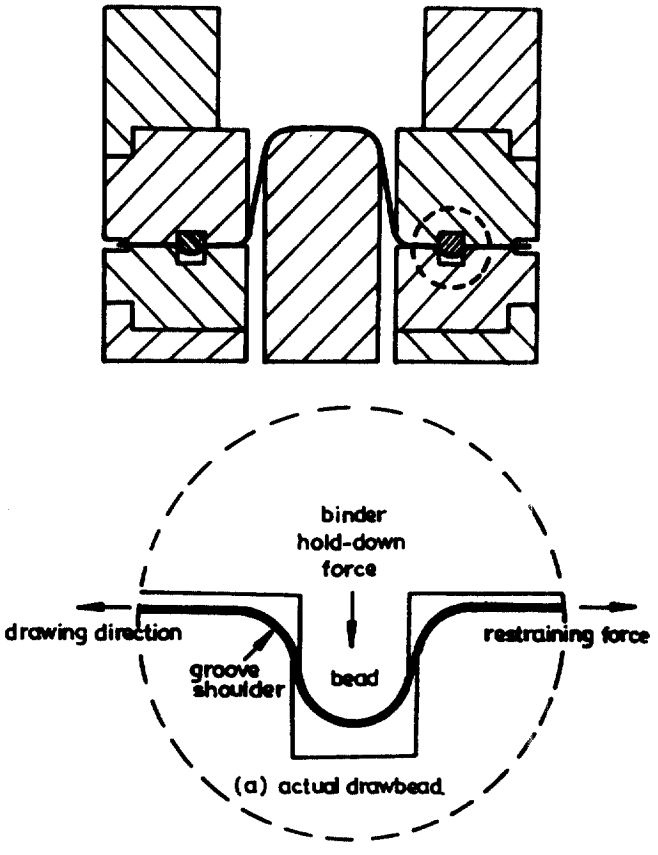

Fig. 1. Stamping process with round drawbeads [1].

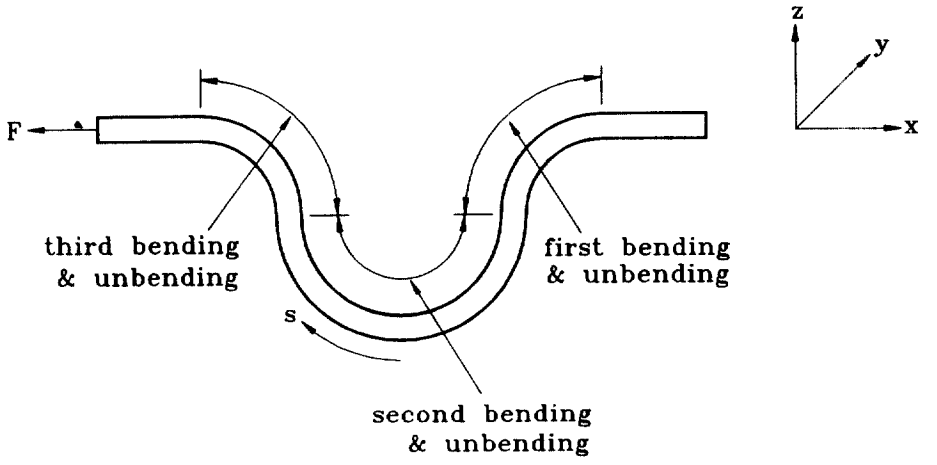

Fig. 2. Bending and unbedening deformations over a drawbead.

the shoulders and bead of the drawbead with rollers to isolate the bending deformation component from the friction component. In addition, Nine [3] found that the Coulomb friction holds for most steels but breaks down for some materials, such as Al 2036-T4, when drawn over a very small drawbead. In his work, Wang [4] proposed a mathematical model of the drawbead forces for calculating the force required to draw sheet metal past a bead of constant cross section. Triantafyllidis *et al.* [5,6] also presented an analytical model and applied the finite element technique to analyze the deformation of sheet metal over the drawbead.

In the present study, a theoretical model based on the virtual work principle for calculating the drawbead restraining force was developed. In this model, the shift of neutral axis is allowed for and the elastic deformation is neglected. The governing equations derived from this model were solved incrementally by an iterative process and a numerical procedure was constructed for the computer programming. In order to validate the theoretical model, the finite element analysis was performed to compare the calculated values with the simulated results. The experimental data published in reference [2] are also adopted to justify the theoretical model.

2. Theoretical model

The configurations of drawbeads used in the stamping operations vary a lot depending on the stamping requirements. In the present study, a typical drawbead which consists of a semicylindrical bead fitting into a groove on the opposite binder surface, as schematically shown in Fig. 1, is adopted to define the configuration of the model to be analyzed. For simplicity, the profile radii of both the groove shoulders and the punch are chosen as the same.

The restraining force builds up from nearly zero at the beginning of drawing and reaches a steady-state value after the first material point completes its travel across the drawbead. In the present study, the restraining force at the steady-state is calculated by a theoretical model. To facilitate the analysis, the following assumptions are made:

1. The drawbead has a constant cross section along the width direction and the sheet metal drawn over the drawbead is under plane strain condition.
2. The plane sections remain plane and perpendicular to the neutral surface during the bending or unbending.
3. The shear stress is negligible.
4. The material is isotropic and strain-rate independent.
5. The Bauschinger effect is neglected during the cyclic bending and unbending processes.
6. The variation of the sheet metal thickness is small during the deformation process and can be neglected.
7. The normal stress in the thickness direction is small compared to the bending stress and can be neglected.
8. The elastic strains are assumed to be relatively small in comparison with the plastic strains in the bending and unbending processes and can be neglected. Hence, the material is assumed to be rigid-plastic.

The repetitive nature of the bending and unbending processes suggests that the analysis may be reduced to a basic one as shown in Fig. 3. According to Swift [7], there exists a sliding process between the bending and the unbending processes in which the mid-surface curvature of the sheet equals κ_o, i.e.,

$$\kappa_o = \frac{1}{R + \frac{t}{2}}, \tag{1}$$

where R is the profile radius of the groove shoulder or the bead, and t is the thickness of the sheet metal. Hence, when the sheet metal is being drawn over the bead, its mid-surface curvature

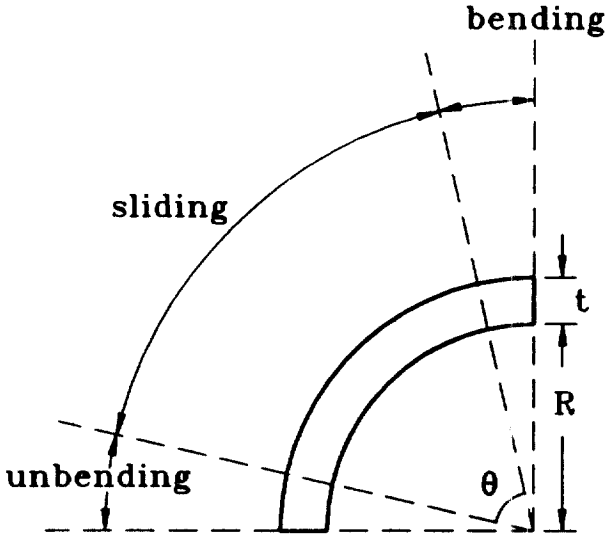

Fig. 3. The basic unit for a bending or an unbending process.

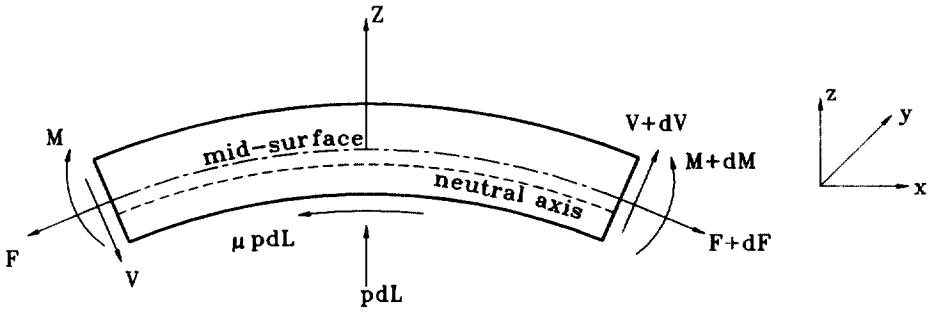

Fig. 4. The free body diagram for an arbitrary differential element.

increases from 0 to κ_o in the bending process, and remains at κ_o in the sliding region, and then decreases from κ_o to 0 in the unbending process, as shown in Fig. 3.

Figure 4 shows the free body diagram for an arbitrary differential element dL of the deformed sheet over the drawbead. Since the neutral axis shifts during the bending process, while the mid-surface is known from the assumption that the variation of the thickness of the sheet metal is negligible, it is convenient to express all the kinematic relations taking the mid-surface as reference, i.e., the origin of the z coordinate is taken on the mid-surface, as shown in Fig. 4. The forces and moments shown in Fig. 4 correspond to a unit width of the sheet metal. If the element is subjected to a virtual displacement δu on the left-hand side, resulting in a virtual displacement $\delta u'$ on the right-hand side, as shown in Fig. 5, then the work (W) done by the external forces is equal to the change of the internal plastic energy dissipation, i.e.,

$$W = Q_{s'} - Q_s, \tag{2}$$

or

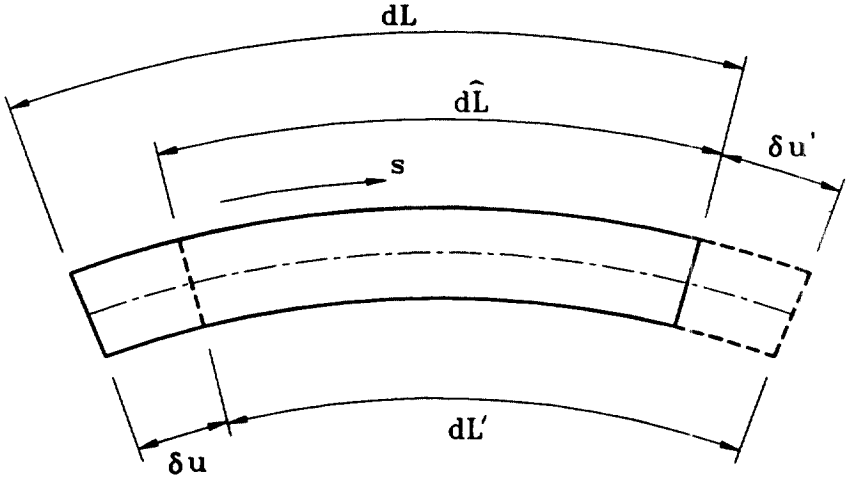

Fig. 5. The differential element subjected to a virtual displacement.

$$(F + dF)\delta u' - F\delta u + (M + dM)\delta\theta' - M\delta\theta - \mu \cdot p \cdot dL \cdot \frac{\delta u + \delta u'}{2} = Q_{s'} - Q_s, \tag{3}$$

where

$\delta\theta$, $\delta\theta'$ = the rotation angles at sections having the displacements δu and $\delta u'$, respectively;

μ = coefficient of Coulomb friction;

p = normal force acting on the element per unit length;

Q_s, $Q_{s'}$ = the plastic energy dissipation in the elements of lengths dL and dL', respectively.

It is to be noted that at the steady-state the overlapped region $d\hat{L}$, as shown in Fig. 5, has the same volume and plastic energy dissipation with respect to the virtual displacement. Consequently, the volume conservation for the plastic deformation implies that

$$t \cdot \delta u = t' \cdot \delta u', \tag{4}$$

where t and t' are the thicknesses of sheet at sections displaced by δu and $\delta u'$, respectively. Since the variation of thickness is negligible, then Eq. (4) can be written as

$$\delta u \approx \delta u' \tag{5}$$

Also, let κ_m and $\kappa_m + d\kappa_m$ be the mid-surface curvatures at the extremities of the considered element, as shown in Fig. 5. The corresponding angles subtended by δu and $\delta u'$ may therefore be given by

$$\delta\theta = \kappa_m \cdot \delta u, \tag{6}$$

$$\delta\theta' = (\kappa_m + d\kappa_m) \cdot \delta u' = (\kappa_m + d\kappa_m) \cdot \delta u.$$

If the plastic energy dissipation in the overlapped region $d\hat{L}$ is denoted by $\hat{Q}$, then the change of the plastic energy dissipation for the element dL at the steady state is

$$Q_{s'} - Q_s = (\hat{Q} + Q_{\delta u'}) - (\hat{Q} + Q_{\delta u}) = Q_{\delta u'} - Q_{\delta u}, \tag{7}$$

where $Q_{\delta u'}$ and $Q_{\delta u}$ are the plastic energy dissipations in the elements of lengths $\delta u'$ and δu, respectively, and may be written as

$$Q_{\delta u'} = \delta u' \int_{-\frac{t}{2}}^{\frac{t}{2}} \int_{0}^{\bar{\epsilon} + d\bar{\epsilon}} \bar{\sigma} d\bar{\epsilon}_z dz = \delta u \int_{-\frac{t}{2}}^{\frac{t}{2}} \int_{0}^{\bar{\epsilon} + d\bar{\epsilon}} \bar{\sigma} d\bar{\epsilon}_z dz \tag{8}$$

$$Q_{\delta u} = \delta u \int_{-\frac{t}{2}}^{\frac{t}{2}} \int_{0}^{\bar{\epsilon}} \bar{\sigma} d\bar{\epsilon}_z dz,$$

where $d\bar{\epsilon}_z$ appearing in the integrals denotes the incremental effective strain in an element at a distance z form the mid-surface; $\bar{\sigma}$ is the effective stress, $\bar{\epsilon}$ is the cumulative effective strain at

the left-hand end, and $d\bar{\epsilon}$ is the change in effective strain between the two ends of the considered element.

Therefore, the change of plastic energy dissipation can be written as

$$Q_{s'} - Q_s = \delta u \int_{-\frac{t}{2}}^{\frac{t}{2}} \int_{\bar{\epsilon}}^{\epsilon + d\bar{\epsilon}} \bar{\sigma} d\bar{\epsilon}_z dz = \delta u \int_{-\frac{t}{2}}^{\frac{t}{2}} \bar{\sigma} d\bar{\epsilon} dz. \tag{9}$$

Substitution of Eqs (5), (6) and (9) into Eq. (3) and dividing it by δu, yields

$$dF = \kappa_m \cdot dM + M \cdot d\kappa_m = \int_{-\frac{t}{2}}^{\frac{t}{2}} \bar{\sigma} d\bar{\epsilon} dz + \mu \cdot p \cdot dL \tag{10}$$

The force and moment at an arbitrary cross section can be calculated from

$$F = \int_{-t/2}^{t/2} \sigma_x dz, \tag{11}$$

and

$$M = \int_{-t/2}^{t/2} \sigma_x (z - z_n) dz, \tag{12}$$

where σ_x is the bending stress at a generic point in the cross section, and z_n is the coordinate of the neutral axis, taking the mid-surface as the datum for the z-coordinate.

Eqs (10)–(12) are the governing equations for solving the problem. However, even though σ_x can be derived from the stress-strain relations, there are still five unknowns, F, M, κ_m, p, and dL, in the equations. In order to obtain a solution to the governing equations, a simple friction model described below will be adopted.

As shown in Fig. 3, the sheet metal is subjected to bending, sliding and unbending when it is being drawn over the groove shoulders or the bead. The regions of the bending and unbending are usually very small compared to the region of sliding. Also, the sheet metal is not completely in contact with the groove shoulder or the bead in the bending and unbending regions. Hence, the frictional force in the bending and unbending regions is negligible, and only the sliding region accounts for the existence of the frictional force.

For the bending and unbending regions, which are assumed to be under the frictionless condition, the second term on the right-hand side of Eq. (10) drops out, giving

$$dF + \kappa_m \cdot dM + M \cdot d\kappa_m = \int_{-\frac{t}{2}}^{\frac{t}{2}} \bar{\sigma} d\bar{\epsilon} dz \tag{13}$$

In consequence, the system equations are solvable. On the other hand, a well-known friction model represented by Fig. 6 is adopted instead of Eq. (10) for the sliding region to simplify the analysis for the change in the restraining force across this region. In the model shown in Fig. 6, it is assumed that no additional plastic deformation occurs in the sliding region, and the sheet metal is subjected to frictional force only. It is easy to show that the relationship between the drawing force, F_2 and the back tension F_1 is

$$F_2 = F_1 \cdot e^{\mu\theta}, \tag{14}$$

where θ is the wrapping angle in radian. The back tension is actually the restraining force at the exit of bending region and the drawing force can be taken as the restraining force at the entry of the unbending region.

In the rigid-plastic deformation, the magnitude of σ_x can be calculated from the effective stress. The effective stress $\bar{\sigma}$ for the plane strain condition and $\sigma_z = 0$ is easily obtained as

$$\bar{\sigma} = \sqrt{\frac{1}{2}[(\sigma_x - \sigma_y)^2 + (\sigma_y - \sigma_z)^2 + (\sigma_z - \sigma_x)^2]} \tag{15}$$

$$= \frac{\sqrt{3}}{2}|\sigma_x|.$$

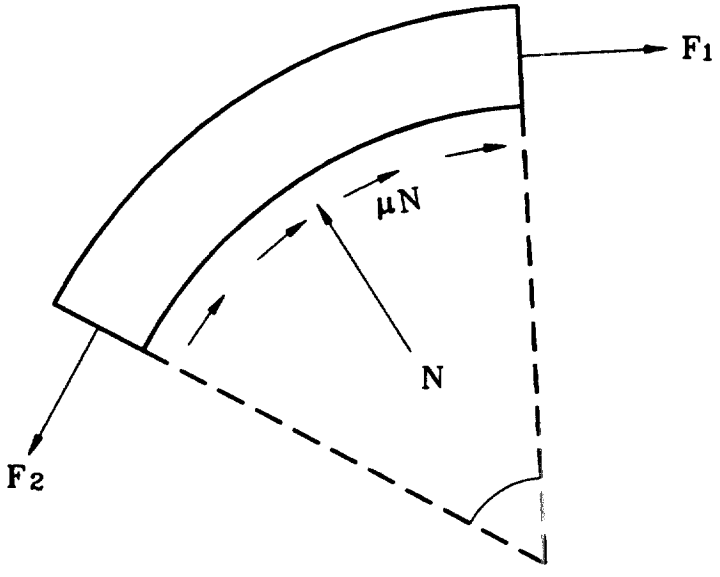

Fig. 6. The free body diagram for a simple friction model.

Use of $\sigma_y = 1/2(\sigma_x + \sigma_z) = 1/2\sigma_x$ has been made in the derivation of Eq. (15). The bending stress is then given by

$$\sigma_x = \begin{cases} + \dfrac{2}{\sqrt{3}} \bar{\sigma}, & z \geq z_n \\ - \dfrac{2}{\sqrt{3}} \bar{\sigma}, & z \leq z_n \end{cases} \tag{16}$$

The effective stress can be determined from the stress-strain relations of the sheet metal. It is assumed, therefore, that the sheet metal work-hardens according to the stress-strain relations:

$$\bar{\sigma} = K\bar{\epsilon}^n, \tag{17}$$

where K is a stress constant and n is the work-hardening exponent, and $\bar{\epsilon}$ is the cumulative effective strain. If a fiber of material is considered along a given z-coordinate, then the cumulative effective strain is the integrated value of the effective incremental strain $d\bar{\epsilon}$. The preservation of volume in the plastic deformation under plane strain condition ($d\epsilon_y = 0$) implies that

$$d\epsilon_z = - d\epsilon_x, \tag{18}$$

and the effective incremental strain associated with the von Mises yield criterion reduces to

$$d\bar{\epsilon} = \sqrt{\frac{2}{9}[(d\epsilon_x - d\epsilon_y)^2 + (d\epsilon_y - d\epsilon_z)^2 + (d\epsilon_z - d\epsilon_x)^2]} \tag{19}$$

$$= \frac{2}{\sqrt{3}} |d\epsilon_x|.$$

The total bending strain ϵ_x of any point at a distance of z form the mid-surface is defined by the following equation under the assumption (2) made above:

$$\epsilon_x = \frac{z - z_n}{\rho_n} = \frac{z - z_n}{\rho_m + z_n}, \tag{20}$$

where ρ_n and ρ_m are the radii of the curvature for the neutral surface and the mid-surface, respectively.

The strain at the mid-surface ($z = 0$) is then given by

$$\epsilon_m = - \frac{z_n}{\rho_m + z_n}, \tag{21}$$

which implies that

$$z_n = - \frac{\rho_m \epsilon_m}{1 + \epsilon_m}. \tag{22}$$

Substituting Eq. (22) into Eq. (20), yields

$$\epsilon_x = \frac{z}{\rho_m}(1 + \epsilon_m) + \epsilon_m \tag{23}$$
$$= \kappa_m \cdot z \cdot (1 + \epsilon_m) + \epsilon_m.$$

Differentiating Eq. (23) results in

$$d\epsilon_x = d\kappa_m \cdot z \cdot (1 + \epsilon_m) + d\epsilon_m \cdot (\kappa_m z + 1). \tag{24}$$

The accumulated effective plastic strain accounts for the entire strain history in a material point which travels from the entry of drawbead to any location in either bending or unbending region. Due to the possibility of unloading, only the incremental form, i.e., Eq. (24), will be used to define the total effective strain as

$$\bar{\epsilon} = \int d\bar{\epsilon} = \frac{2}{\sqrt{3}} \int |\{d\kappa_m \cdot z \cdot (1 + \epsilon_m) + d\epsilon_m \cdot (\kappa_m z + 1)\}|. \tag{25}$$

It can be seen that a closed-form solution to Eq. (13) does not seem to exist. Hence, the system of governing equations will be solved numerically, using a step-by-step process.

3. Numerical procedure

A numerical procedure is constructed to solve the system of Eq. (11) to Eq. (25), which forms the basis of the analysis for the drawbead restraining force. To start with the numerical procedure, the region where bending or unbending takes place must be defined. Since the curvature of the mid-surface is a function of the curvilinear coordinate s, the bending (or unbending) process can be clearly defined as beginning at $\kappa_m = 0$ (or $\kappa_m = \kappa_o$) and ending with $\kappa_m = \kappa_o$ (or $\kappa_m = 0$). It is therefore convenient to treat κ_m as the independent variable instead of the curvilinear coordinate s.

The moment M, force F, mid-surface curvature κ_m, and the bending strain ϵ_x are all set to zero at the entry of the drawbead as the boundary conditions for the numerical procedure. It is to be noted that the numerical procedure can also take the back tension at the entry of the drawbead as a boundary condition if the back tension is applied. However, since the main purpose of this paper is to calculate the restraining force produced by the drawbead when the sheet metal is drawn through, the back tension is not considered here.

An equal increment of the curvature of the mid-surface is set to

$$\Delta\kappa = \frac{\kappa_0}{N}, \tag{26}$$

where N is the number of increments. In the bending region, the curvature of the mid-surface

varies according to a typical increment from $\kappa_m^{(i)}$ to $\kappa_m^{(i+1)}$, with $\kappa_m^{(0)} = 0$. For each $\kappa_m^{(i+1)}$, the numerical procedure begins by assigning a trial value for ϵ_m. With $d\kappa_m$ and $d\epsilon_m$ given, the bending strain increment $d\epsilon_x$ for a material point at a distance z is calculated from Eq. (24). The location of the neutral axis is determined from Eq. (22), and the effective incremental strain $d\bar{\epsilon}$ is obtained from Eq. (19). Adding the effective incremental strain to the effective strain at the step (i) results in the effective strain $\bar{\epsilon}$ at the step $(i + 1)$, from which the effective stress $\bar{\sigma}$ can be calculated from Eq. (17). Subsequently, the bending stress, σ_x is found according to Eq. (16).

In order to determine the sign of σ_x and calculate the integral in the z direction, the thickness of sheet metal is equally divided into a number of layers. The location of each layer is defined by the z-coordinate measured from the centerline of the layer. The stresses and strains in each layer are considered to be constant. With this division in the thickness, the force and moment can be calculated form Eqs (11) and (12), respectively, and the plastic energy dissipation given by the integral in Eq. (13) is also obtained. The magnitudes of dF, dM, and $d\kappa_m$ can be easily calculated from their values at i-th and (i + 1)-th steps. If the calculated quantities satisfy Eq. (13), then the calculation for the current step (i + 1) is completed. Otherwise, a new value of ϵ_m should be assigned and the above procedure iterates upon until Eq. (13) is satisfied. At the end of the bending region, κ_m reaches the value of κ_0, and the calculated quantities then serve as the initial conditions for the subsequent sliding region.

In the sliding region, no additional plastic deformation occurs, and only the frictional force accounts for the force change. Since the bending and unbending regions are usually very small, a wrapping angle of 80° is assumed for the sliding region over the bead or the groove shoulders. The drawing force at the end of sliding region can then be calculated from Eq. (14). The drawing force and the calculated quantities obtained in the bending region provide the initial conditions for the subsequent unbending region.

The iterative procedure for the unbending process is similar to those applied to the bending process, except that the mid-surface curvature starts from κ_0 and decreases to zero at the end of the process.

The sheet metal is subjected to three repeated cycles when it is drawn over the draw-bead as shown in Fig. 2. Each cycle consists of bending, sliding and unbending as indicated in Fig. 3. To obtain the restraining force produced by the drawbead, the above iterative procedure needs to be repeated twice more. It is to be noted that the effective strain is accumulated with each increment, and the work-hardening property is preserved. Also, it is expected that the accuracy of the calculated force can be improved if both the number of increments and the number of layers in the thickness direction are increased.

4. Finite element model

A simple finite element model, as shown in Fig. 7, was constructed to calculate the restraining force produced by the drawbead. In this model, the sheet metal is initially placed horizontally and is held on by a frictionless device. The bead is then moved down to bend the sheet metal while the leading end of the sheet metal is fixed. The bead travels through a distance at which the centers of curvature for both the groove shoulders and the bead are at the same height, as shown in Fig. 7. The boundary condition at the leading end of the sheet metal is then released

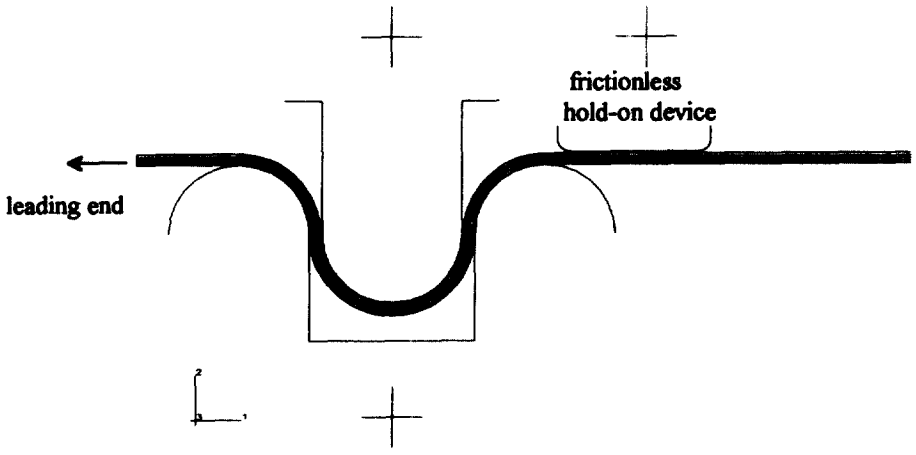

Fig. 7. The finite element model for drawbead force simulations.

and the sheet metal is pulled to the left until a steady-state is obtained. The steady-state is indicated when the pulling force reaches a constant value which is also the restraining force produced by the drawbead.

In order to compare the simulated results with the experimental data obtained by Nine [2], A-K steel and rimmed steel are used in the simulations and the material constants of these metals are those given in Table 1 of reference [2]. The radii of both the groove shoulders and the bead used in the simulations are 5.5 mm. Both the frictionless condition and the coefficient of Coulomb friction equal to 0.1 at the interfaces between the sheet metal and the drawbead are simulated.

The elastic-plastic finite element program ABAQUS was adopted to perform the simulations. In the simulations, the drawbead is treated as rigid and four layers of elements are assigned in the thickness direction of the sheet metal. The four-node plane strain element is used to construct the finite element mesh for the sheet metal.

5. Results and discussions

With the use of the same conditions as those set for the finite element simulations, the restraining forces were calculated following the numerical procedure based on the proposed model. In each calculation, the curvature increment $\Delta\kappa = \kappa_0/200$ was assigned in the numerical procedure, and the thickness of sheet metal was equally divided into 40 layers to perform the evaluations of σ_x and the integrals involved in the system equations. Both the finite element simulations and the present theoretical model consider the sheet metal drawn over the drawbead with and without friction. The calculated values of the restraining forces based on the proposed method are compared mainly with those obtained by the finite element simulations. The experimental data [2] for the frictionless case are also used for comparison with the present theory under identical conditions.

Under the frictionless conditions, the theoretical, finite element and experimental results obtained for A-K steel and rimmed steel with thicknesses of 0.76 mm, 0.86 mm and 0.96 mm are

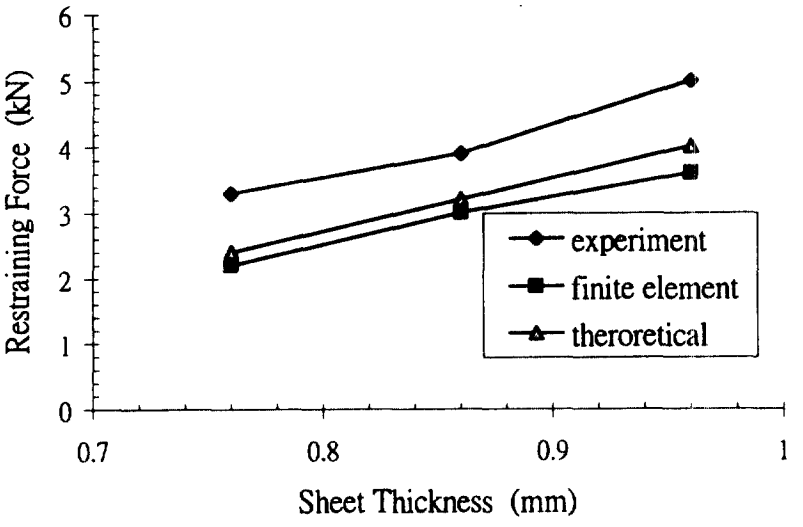

Fig. 8. Restraining forces versus sheet thicknesses for A-K steel ($\mu = 0$).

shown in Figs 8 and 9, respectively. It is seen in both figures that the restraining forces obtained from the present theoretical model and the finite element simulations agree very well but are consistently small compared to the experimental data. This difference is partly due to the effect of strain-rate sensitivity of the material properties being neglected in both the theoretical model and the finite element simulations. The sheet metal was drawn over the drawbead by a speed of 85 mm per second in the experiments which is much higher than the speed used in the tensile tests to obtain the material properties of the sheet metal. Nine [2] also showed that the restraining forces for A-K steel and rimmed steel could increase by about 25% over the range of strain rates from 0.035/sec to 35/sec. The neglect of the Bauschinger effect in both the theoretical model and

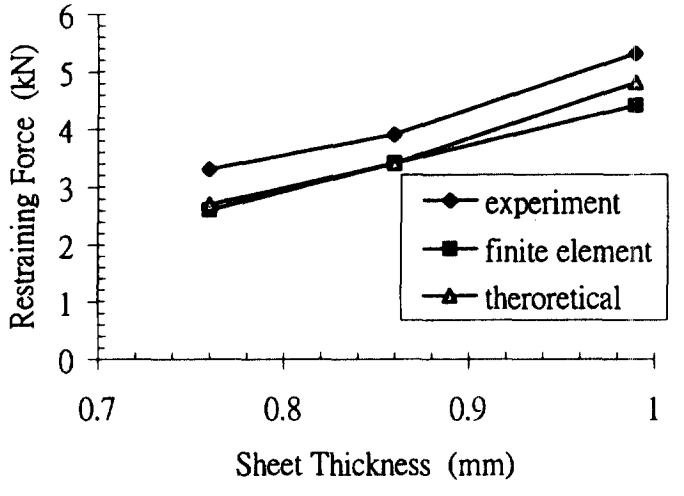

Fig. 9. Restraining forces versus sheet thicknesses for rimmed steel ($\mu = 0$).

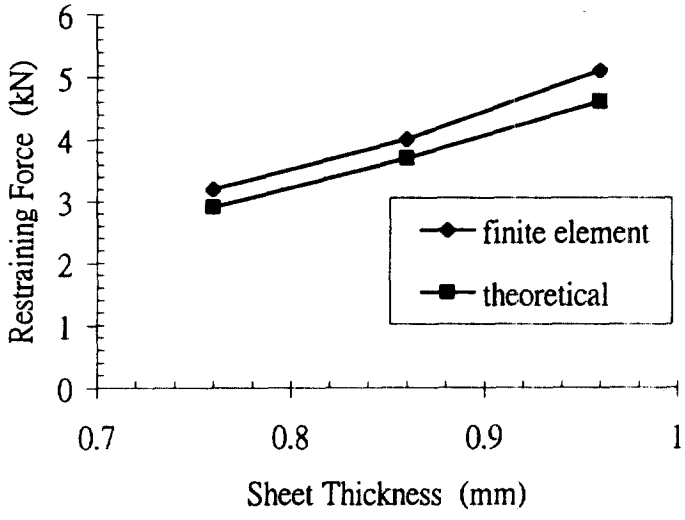

Fig. 10. Restraining forces versus sheet thicknesses for A-K steel ($\mu = 0.1$).

the finite element simulations is considered to be another reason for the difference, since the sheet metal is subjected to cyclic bending and unbending deformations when passing through the drawbead. Also, the extraction of the frictional part of the restraining force from the total is achieved by replacing the shoulders and bead with rollers in the experiments. This device cannot make the drawbead tests completely free from friction and the small amount of frictional force accounts for the difference as well.

The results obtained from the theoretical model and the finite element simulations for A-K steel and rimmed steel under the coefficient of friction of 0.1 are shown in Fig. 10 and Fig. 11, respectively. It is noticed in both figures that the restraining forces calculated from the theoretical

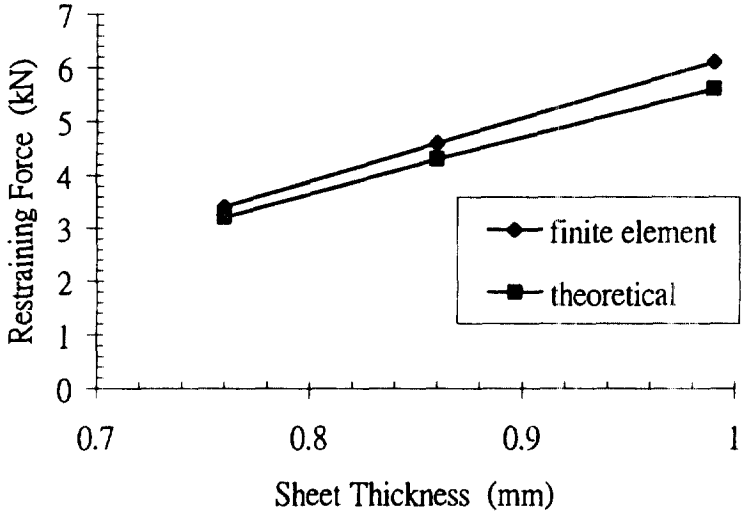

Fig. 11. Restraining forces versus sheet thicknesses for rimmed steel ($\mu = 0.1$).

model agree with the simulated results in trend but underestimate the values by about 10% for both the A-K steel and rimmed steel. This discrepency is obviously due to the assumed friction model which implies that the friction occurs only in the sliding region of the sheet metal. However, since the difference is not so significant, the calculated results suggest that the proposed friction model is satisfactory to a large extent.

The percentage of the restraining forces due to friction to the total is also calculated for A-K steel and rimmed steel and the results are shown in Fig. 12. It is seen in Fig. 12 that about 33% of the total restraining force is due to friction for A-K steel and about 35% for rimmed steel under the coefficient of friction of 0.1. It can be expected that the percentage difference will vary with coefficient of friction, radius of the drawbead and the material properties of sheet metal.

It is also noted in Figs 8–11 that the restraining force increases as the thickness of the sheet metal increases. Comparison of the results shown in Fig. 10 with those in Fig. 11 also indicates that the restraining forces increase as the stress constant K increases.

6. Concluding remarks

The assumption that the deformation of the sheet metal drawn over the groove shoulders or bead can be divided into bending, sliding and unbending regions has been shown to be reasonable for the calculation of the restraining force under the frictionless condition, while the assumed friction model leads to a small difference between the simulated results and the calculated values. But the relatively small discrepency suggests that the simple friction model is satisfactory to a large extent. Also, since the theoretical model allows the shift of the neutral axis, the location of the neutral axis along the deformed sheet metal can be found by using the numerical procedure,

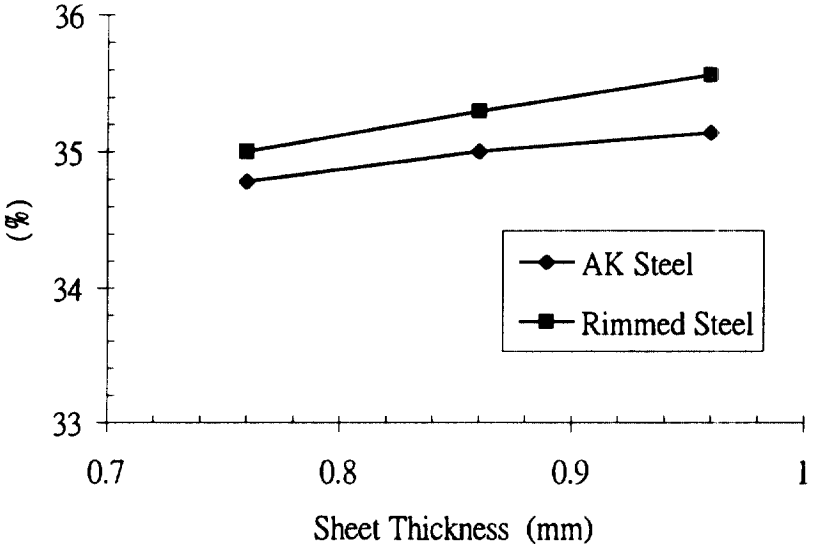

Fig. 12. The percentage of the restraining force due to friction.

which provides very useful information for a better understanding of the deformation mechanism of the sheet metal subjected to cyclic bending and unbending processes.

As for the industrial applications, the die designers can easily write a simple computer program according to the proposed model to calculate the restraining force produced by a circular drawbead with various groove shoulder radii.

In conclusion, the calculated restraining forces are found to be in general agreement with the finite element results and the experimental data, and the proposed theoretical model is therefore validated. It is obvious that the proposed model can be extended to calculate the drawbead force produced by any other shapes of drawbead as long as the bending-sliding regions and the bending curvatures are well defined. However, it is also to be noted that the present model is only valid for the steady-state deformation of the sheet metal passing through the drawbead. For the future extension to include the non-steady-state deformation, the formulation for the variation of plastic energy dissipation needs to be modified.

Acknowledgements

The authors wish to thank the National Science Council of the Republic of China for their grant under the project NSC85-2212-E-002-064, which makes this research possible.

References

[1] N.M. Wang, V.C. Shah, Drawbead and performance, J. Mater. Shaping Tech. 9 (1991) 21–26.
[2] H.D. Nine, Drawbead forces in sheet metal forming, in: D.P. Koistinen, N.M. Wang (Eds.), Mechanics of Sheet Metal Forming, Plenum Press, New York, 1978, pp. 179–211.
[3] H.D. Nine, The applicability of Coulomb's friction law to drawbeads in sheet metal forming, J. Applied Metal Working 2 (3) (1982) 200–210.
[4] N.M. Wang, A mathematical model of drawbead forces in sheet metal forming, J. Applied Metal Working 2 (3) (1982) 193–199.
[5] N. Triantafyllidis, B. Maker, S.K. Samanta, An analysis of drawbeads in sheet metal forming: Part I - problem formulation, J. Eng. Mater. Tech. 108 (1986) 321–327.
[6] B. Maker, S.K. Samanta, G. Grab, N. Triantafyllidis, An analysis of drawbeads in sheet metal forming: Part II - experimental verification, J. Eng. Mater. Tech. 109 (1987) 164–170.
[7] H.W. Swift, Plastic bending under tension, Engineering 166 (1948) 333–359.